Peer-reviewed version available at Materials 2018, 11, 1890; doi:10.3390/ma11101890

Article

Analysis of Bearing Capacity of Helical Pile with Hexagon Joints

Daehyeon Kim [1], Kyemoon Baek [2] and Kyungho Park [3,*]

[1] Department of Civil Engineering, Chosun University, Gwangju 61452, Korea; dkimgeo@chosun.ac.kr
[2] President, SOIL-ROCK E&G CO., LTD., Jeollabuk-do 55340, Korea; soil-rock@hanmail.net
[3] Director of Research, SOIL-ROCK E&G CO., LTD., Jeollabuk-do 55340, Korea; munhakng@nate.com

* Correspondence: munhakng@nate.com; Tel.: +82-063-255-3942

Abstract: This study aims to improve the shaft with hexagon joints to be a type not requiring welding or bolts in the static load test. In order to evaluate the bearing capacity of helical piles, two sites were selected to conduct pile installation for the field test and the pile load test. For the pile load test, the static pile load test and the dynamic pile load test were carried out, and torque was measured during pile installation for the field test to compare and analyze expected bearing capacity and thus assess the feasibility of the method for estimating the bearing capacity. The field pile load test revealed the bearing capacity of the gravity grout pile was the same or greater than 600kN in the static pile load test in accordance with AC 358 Code. The non-grout pile showed the bearing capacity the same or smaller than 600kN, suggesting gravity grouting is required. Moreover, the field pile load test was used to establish the bearing capacity equation considering the torque in pile installation, and a small number of samples were used to establish the equation which can be used as a basic data.

Keywords: Hexagon Joint; Helical Pile; Bearing Capacity; Static Pile Load Test; Dynamic Pile Load

1. Introduction

1.1. Background and Objective

The helical pile is a non-displacement pile foundation to implement bearing capacity by attaching at least one helix plate to a hollow shaft to be rotary-penetrated into the ground. The helical pile can be installed with low-noise and low-vibration performance by means of a torque machine for guiding rotary penetration to a target depth. This is a pile that can be installed with a comparatively small machine and in locations with limited installation spaces, for example, commercial buildings or historic sites. The helical pile is better than conventional steel pipe piles in terms of bearing capacity for the material costs because helix plates of a diameter larger than the hollow shaft are attached thereto to allow each helix plate to implement point bearing capacity thereof[1].

Other countries than Korea have used the helical piles in various construction sites for a long time. However, the advantages of the helical piles are not known well in Korea; there are prior studies on screw anchor piles similar to the shape of helical piles [2]; and another prior comparison and analysis is known about the bearing capacity of the installed helical piles compared to the equation for estimating bearing capacity [3].

Most helical piles have a standardized shape, and the bearing capacity depending on the hollow diameter and the helix diameter have been studied. Although most helical piles are installed by means of bolts and on-site welding to implement simple installation, there are issues involved in poor verticality in pile installation, worker's safety related to bolt damages in rotary penetration, on-site labor cost for welders and an increase in the installation period for the additional welding process,

and further quality control for the welded locations. Therefore, it is required to apply a new type of joints to address the aforementioned issues.

Furthermore, because the shape of helical piles is different from that of the conventional piles, using conventional equations is not ideal for high reliability, and it is necessary to examine the bearing capacity of helical piles installed in the Korean ground to use the conventional equations [4].

Therefore, in this study, a hollow shaft model is rolled with a hexagon joints to improve it as a fit type not requiring welding or bolts. Two sites were selected to apply the pile to the Korean ground and conduct piling for the field test and the load test. During the field pile load test, the result of the static pile load test and the dynamic pile load test was compared with the bearing capacity estimated by measuring the torque in the pile installation process for the field test to examine the feasibility of the method for estimating the bearing capacity.

1.2. Prior Studies

The helical piles were invented by the Irish civil engineer Alexander Mitchell in 1836 to reinforce the foundation of houses. The helical piles had been used in the UK since 1853, and the US generally as a foundation of lightweight houses between 1850 and 1890. After the period, the helical piles were used for the purpose similar to anchors until 1985. At present, they are generally used for transmission tower foundations, foundations for small- and medium-sized buildings and roads, and slope stabilization [5].

The helical piles have been studied, focusing on assessing pull-out performance of anchors to use them as an anchor. [6] studied the behavior of ground around the anchor by rotary penetration (rotary penetration) under extreme loads to establish an equation for calculating pull-out forces of the anchor, and [7] calculated the extreme pull-out forces through the field pull-out test.

[8] announced the best pitch ratio to allow the soil mass between the helixes to behave as one mass through the indoor test. [9] studied the pull-out resistance characteristics of a single- and multi-helix anchors installed in sandy soil and clay soil, and announced an empirical equation for calculating the penetration depth of the helical anchor, the screw wing diameter, and the pull-out resistance depending on ground conditions.

[10] studied the effect of the shaping factor determining the helical anchor pull-out forces on the pull-out forces. [11] studied numerical analysis of extreme pull-out resistance of helical anchors installed in clay soil, and examined the relation between the extreme pull-out resistance and the specifications for installing helical piles.

Recently, the helical piles have been studied about the behavior of bearing capacity thereof. [10, 12] evaluated the bearing capacity of helical piles and the behavior characteristics of helix plates in relation to the pitch ratio, and [9] recommended the cylindrical shear method for evaluating the bearing capacity of multi-helical piles.

[5] established an equation for the average diameter relative to the unit weight of helical piles for the critical depth thereof, and [6] said that the scale of lateral earth pressure on the helical piles is related to the initial relative density of the ground, and calculated the lateral earth pressure coefficient.

[13] studied friction occurring in the shaft of helical piles to confirm the adhesive force occurring in the shaft of helical piles in the clean coarse sandy ground, and [14] said that the shaft adhesion force must be limited although it can be used.

[15] said that the relation between the rolling resistance and bearing capacity of helical piles depends on the shaft diameter, and [16] evaluated the relation between the rolling resistance and bearing capacity during pile installation by using the Law of Conservation of Energy.

In Korea, [2] studied the characteristics of screw anchor pile pull-out resistance, and conducted indoor test with different geometrical features, for example, different helix plate diameters and pitches. The result shows the pull-out resistance increases as the helix plate increases, but is constant at sizes greater than a specific size.

Peer-reviewed version available at Materials 2018, 11, 1890; doi:10.3390/ma11101890

[17] compared the field load test result with the bearing capacity by the Individual bearing method, Cylindrical shear method, and the Torque correlation method. The comparison shows that the Torque correlation method implements the highest correlation.

[18] said that 1,000.0kN of bearing capacity is ensured where the helical pile is settled in the hard ground (rock), and [19] evaluated field applicability to find out that the result of Individual bearing method is similar to the result of field pile load test.

Examination of prior studies on helical piles shows that geometrical features of helical piles and bearing performances thereof have been studied through indoor test and pile installation for the field test. However, the joints have not been studied much in the prior studies, and the bearing performance by using the Torque correlation method as well. Therefore, in this study, a schematic bearing capacity theory equation is suggested through the static load and dynamic load test with helical piles installed for the field test and the load test for 30 hexagon joints in 2 sites, and torques were measured to examine bearing performance of the helical piles.

2. Bearing Capacity Theory and Design of Helical Pile

A helical pile is shaped to have helix plates attached to the hollow shaft and with a diameter greater than the hollow shaft, and respective helix plates implement point bearing capacity in addition to skin friction of the shaft to achieve bearing capacity. The exemplary applicable methods for calculating the bearing capacity of helical piles include the Individual bearing method, Cylindrical shear method, and Torque correlation method. Moreover, the Torque correlation method determines the bearing capacity coefficients through the force of rotary penetration into the ground during installation, and is a method for calculating extreme bearing capacity.

The bearing performance of helical piles is classified into point bearing capacity and skin friction. In particular, the point bearing capacity is calculated in the Individual bearing method and Cylindrical shear method, and determined by helix plate pitches. Where the pitches are at least 2 to 3D of the helix plate diameter D, the piles show the bearing performance of the Individual bearing method. However, where they are at most 2 to 3D of the helix plate diameter D, they show the bearing performance of the Cylindrical shear method [5, 20, 21]. Moreover, skin friction can be calculated by means of skin friction between the upper shaft of the helix plates and the ground.

2.1. Details of Helical Pile

Figure 1(a) shows a hexagon joint model, and Figure 1(b) shows the concept of load transfer in which load transfer moves to the inner pile through the outer pile when the top load is applied. Where there is no gravity grout plate (PL), the outer pile goes through the curves of the inner pile to generate plastic displacement. Therefore, the gravity grout PL was made to support the movement and conduct gravity grouting.

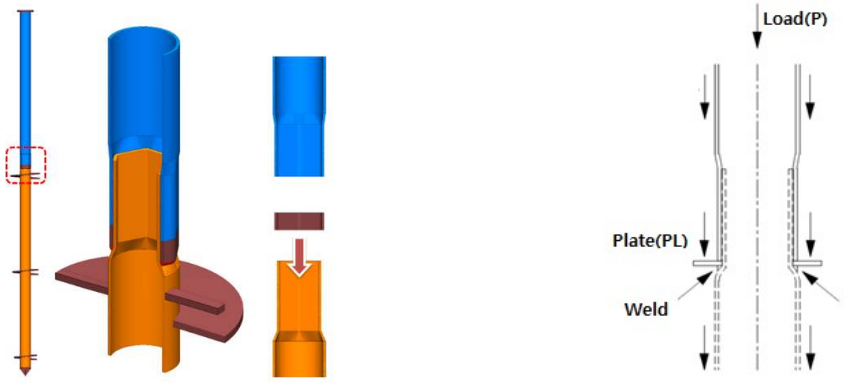

(**a**) (**b**)

Figure 1. Designing hexagon joint: (a) Hexagon joint model; (b) Concept of load transfer

Preprints (www.preprints.org) | NOT PEER-REVIEWED | Posted: 31 July 2018 doi:10.20944/preprints201807.0617.v1

Peer-reviewed version available at Materials 2018, 11, 1890; doi:10.3390/ma11101890

In this study, the helix plate pitch was determined to be 3D shown in Figure 2, designed in the Individual bearing method through field ground survey to determine the target load of 600.0kN. Although the target load of 600.0kN is supported by the point bearing capacity and the skin friction, the ratio of point bearing capacity to the bearing capacity of skin friction is different depending on ground conditions.

While greater helix plate pitches achieve even deeper rotary penetration, rolling resistance is greater in the ground. Therefore, 75mm (3 inches) suggested by [22] was employed, and the helix plate was installed in the direction perpendicular to the hollow shaft. Table 1 illustrates the specifications and target load of the helix plate of helical piles.

Table 1. Specifications and target load of helix plate.

Category	Plate diameter (D)	Steel pipe diameter (d)	Net sectional area of plate	Area ratio of plate (%)	Yield strength (MPa)	Target load (kN)	Arm distance (mm)
D1	350mm	165.2mm	0.075 ㎡	23.7	315	142	92.4
D2	400mm		0.104 ㎡	32.8	315	197	117.4
D3	450mm		0.138 ㎡	43.5	315	261	142.4

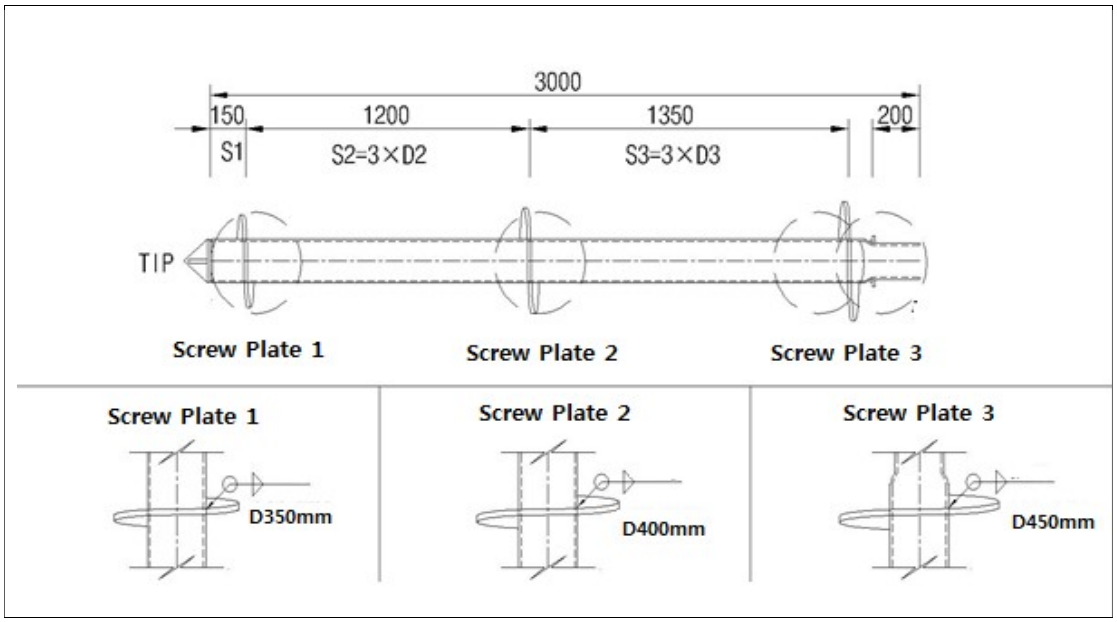

Figure 2. End of helical pile shown in detail.

3. Pile Installation for Field Test and Result

3.1. Planning Pile Installation for Field Test

Pile installation for the field test was conducted in the local road construction sites of Site-1 (NH-1, 2) shown in Figure 3, and Site-2 (NH-3, 4) shown in Figure 4 for this study. The geological feature of Site-1 and Site-2 is a typical Korean ground configured with sedimentary soil (reclaimed soil), alluvial beds, weathered rock soil, and weathered rock, and the sites were selected as areas for piling for the field test.

Preprints (www.preprints.org) | NOT PEER-REVIEWED | Posted: 31 July 2018 doi:10.20944/preprints201807.0617.v1

Peer-reviewed version available at Materials 2018, 11, 1890; doi:10.3390/ma11101890

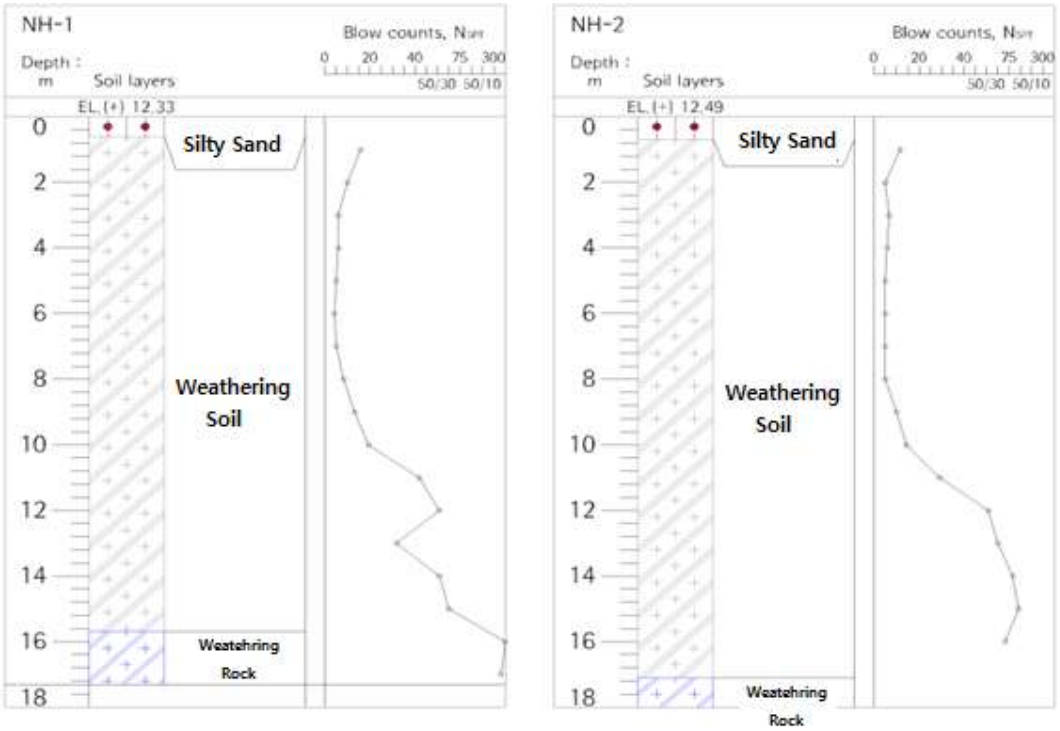

Figure 3. Sectional view of Site-1 stratum.

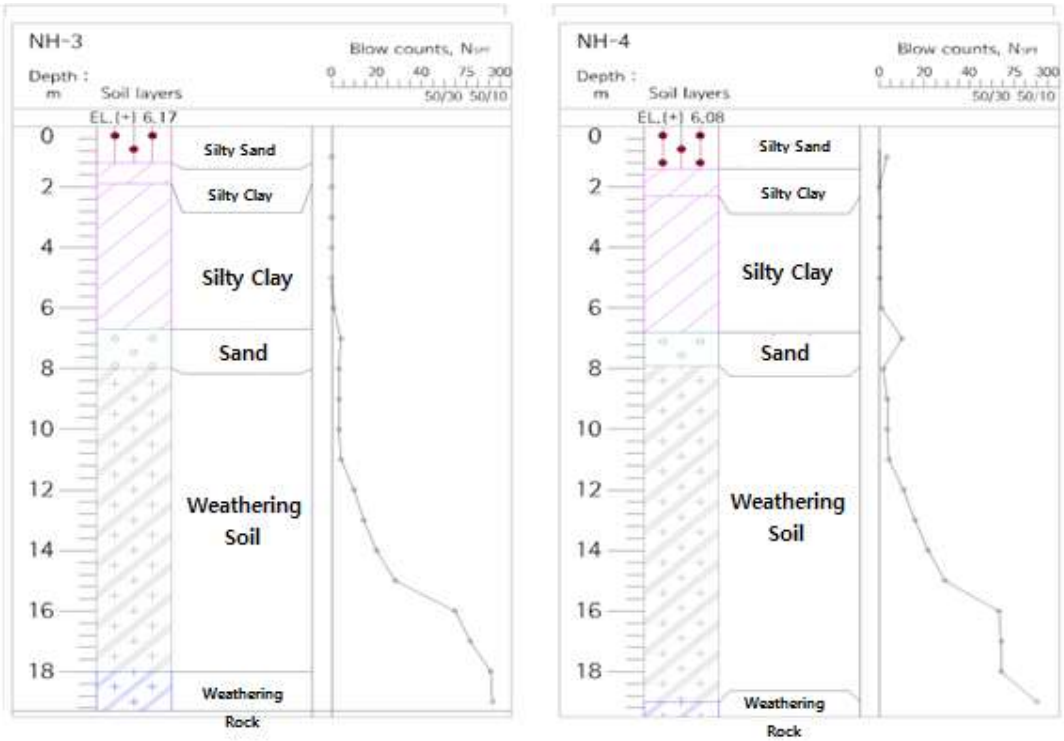

Figure 4. Sectional view of Site-2 stratum.

Fifteen piles were installed in the sites for the field test, respectively, in order to examine the bearing capacity behavior depending on pile types and grout, and water/cement (W/C) in grouting

Preprints (www.preprints.org) | NOT PEER-REVIEWED | Posted: 31 July 2018 doi:10.20944/preprints201807.0617.v1

Peer-reviewed version available at Materials 2018, 11, 1890; doi:10.3390/ma11101890

was planned to be 80%, and the compressive, dynamic pile load test was conducted to examine the bearing capacity behavior.

Figure 5 shows a pile placement plan for the field pile installation test. Fifteen piles (3×5) were placed in the test sites, respectively, the pitch between piles was 2m, and static piles were installed in the middle column to use the pull-out piles as a reaction pile in the static load test.

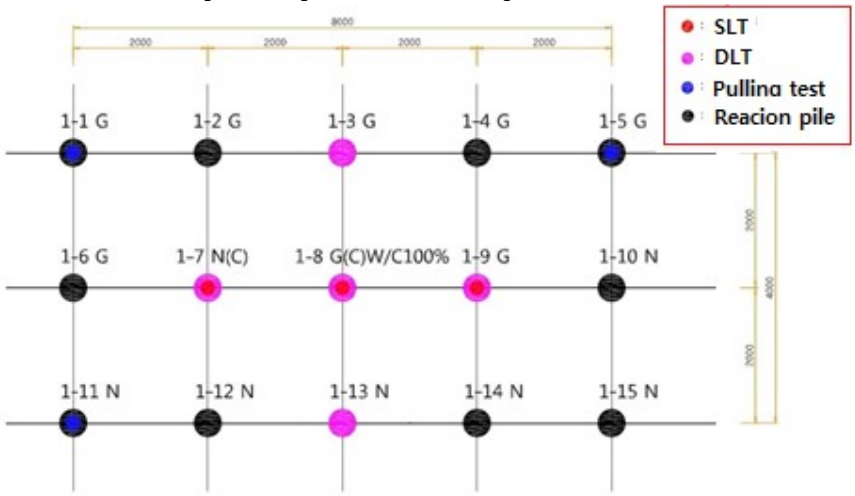

(**a**)

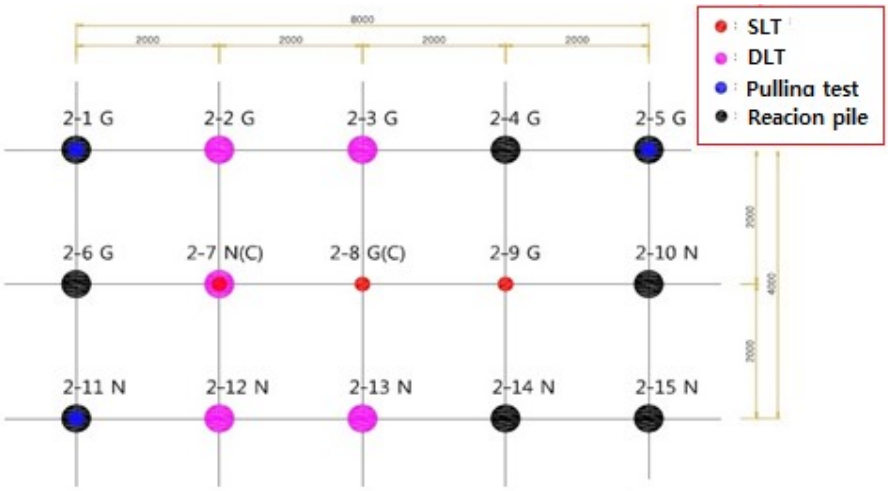

(**b**)

Figure 5. Placing pile for the field pile installation test: (a) Site-1 (15 piles); (b) Site-2 (15 piles)

3.2. Result of Static Pile Load Test

Each country has its own standard for the safety factor applied to evaluating allowable bearing capacity using the static load test, and different standards should be applied depending on pile types and installation methods. The design bearing capacity of the helical pile used in this study was 600.0kN, which was calculated in the Individual bearing method through exhaustive ground inspection. Therefore, the bearing capacity according to different regulations applied to evaluating the allowable bearing capacity was compared with the bearing capacity in conventional methods in consideration of characteristics of the helical pile.

Figure 6 shows bearing capacity evaluation according to the helix plate standard using the Davisson`s method. Prior studies in other countries show the bearing capacity values the closest to 600.0kN designed in the Individual bearing method while applying AC 358 Code. Therefore, for the load test in this study, AC 358 Code was applied to evaluate bearing capacity.

The static load test was conducted in the static load test method using pull-out resistance of surrounding piles, the load which is three times the target load was determined as the maximum test load to conduct the Quick Maintained-Load Test in order to determine the fracture load.

The static load test conducted for the Site-1 and Site-2 test piles shows the allowable bearing capacity of the gravity grout piles was 678.6~800kN/pile in Site-1, and 627.3 ~664.7kN/pile in Site-2. In the non-grout piles, the allowable bearing capacity was 553.3kN/pile and 554.2kN/pile in Sites-1 and 2, respectively, suggesting that gravity grout is required in installing helical piles. The gravity grout piles showed 1 inch (25.4mm) which is an allowable settlement standard when the target load of 600.0kN was given, suggesting stability for settlement.

In particular, the pile 1-#8 considered installed in weathered rock experienced a settlement not greater than the allowable settlement (25.4mm) although the given load was twice the target load, suggesting that even greater allowable bearing capacity can be applied where the helical pile are installed in weathered rock. Therefore, it is necessary to further study how to establish a method for installing the helical piles in weathered rocks to achieve even greater target loads.

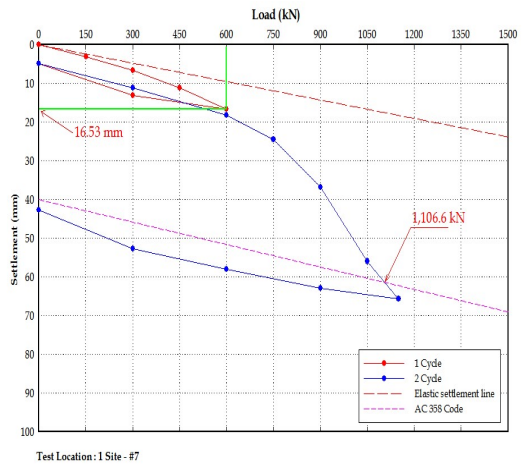

(a)

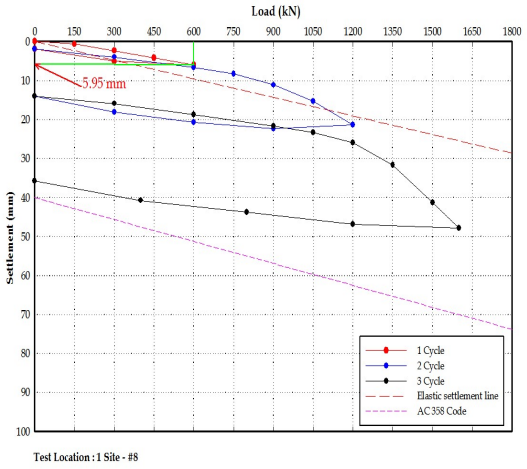

(b)

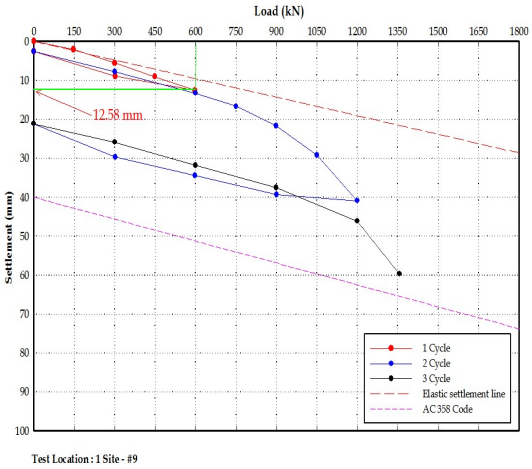

(c)

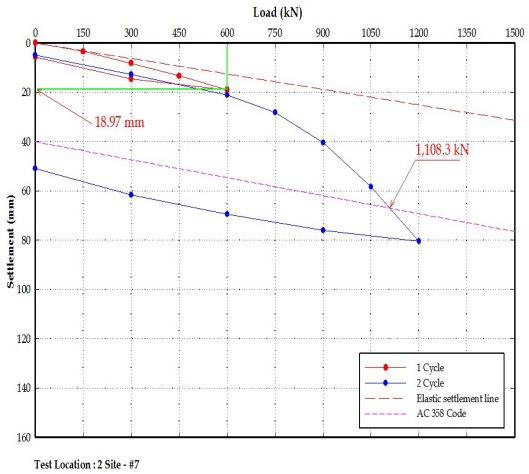

(d)

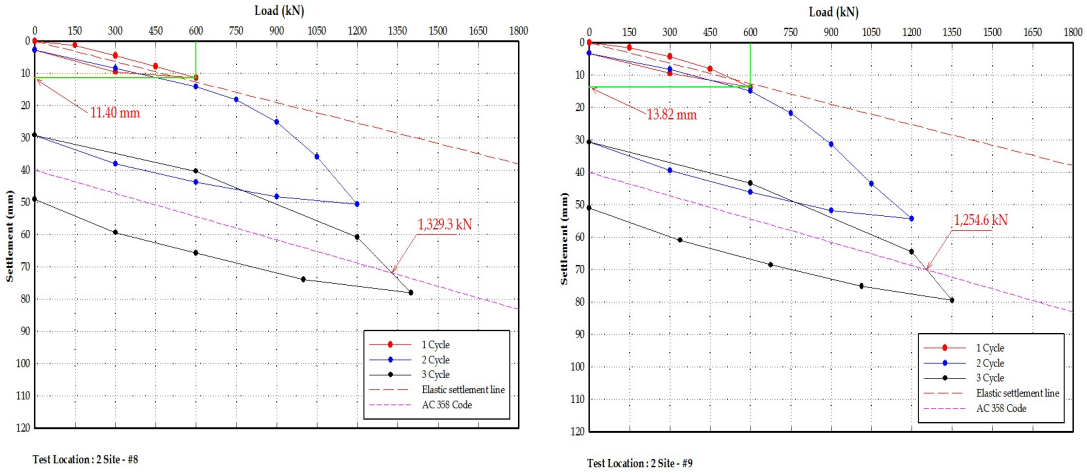

(e) (f)

Figure 6. Static load test result for each site: (a) Site–1 #7; (b) Site–1 #8; (c) Site–1 #9; (d) Site–2 #7; (e) Site–2 #8; (f) Site–2 #9.

Table 2 illustrates the result of static load test in each site.

Table 2. Result of static load test in each site.

Site	Test location	Penetration depth (m)	Max. test load (kN)	Total settlement (mm)	Net settlement (mm)	Fracture load (kN)	Allowable bearing capacity (kN/pile)			Grout
							Safety factor (AC 358)	Allowable bearing capacity	Design load	
Site-1	#7	12.10	1,150.0	65.73	42.67	1,106.6	2.0	553.3	600.0	×
	#8	12.10	1,600.0	47.81	35.71	1,600.0	2.0	800.0	600.0	100%
	#9	12.00	1,356.0	59.67	-	1,356.0	2.0	678.0	600.0	80%
Site-2	#7	15.90	1,200.0	80.51	50.88	1,108.3	2.0	554.2	600.0	×
	#8	16.10	1,400.0	78.00	49.06	1,329.3	2.0	664.7	600.0	80%
	#9	16.05	1,350.0	79.51	50.97	1,254.6	2.0	627.3	600.0	80%

3.3 Analysis of Dynamic Pile Load Test Result

Table 3 illustrates the result of CAPWAP analysis.

The Restrike method was used for the respective tested piles, and a drop hammer with a ram weight of 23.0kN was used in the dynamic pile load test to minimize the number of test strikes and thus minimize ground disturbance in the test.

The dynamic pile load test for the piles in Site-1 shows the allowable bearing capacity was 625.0~817.9kN/pile for the gravity grout piles, and the allowable bearing capacity was 503.4~619.7kN/pile for the non-grout piles, suggesting gravity grouting is required in installing helical piles.

The dynamic pile load test for the piles in Site-2 shows the allowable bearing capacity was 620.7~674.6kN/pile for the gravity grout piles, and the allowable bearing capacity was 426.8~563.9kN/pile for the non-grout piles, suggesting gravity grouting is required in installing helical piles.

Table 3. Result of dynamic pile load test in each site.

Site	Pile No.	Test	Allowable bearing capacity (kN/pile)				Grout
			DFI, Perko (F.S=1.5)	A.P.C (F.S=1.8)	Application (Min.)	Target load	
Site -1	#3	R	810.5	675.4	675.4	600.0	O
	#7	R	604.1	503.4	503.4	600.0	×
	#8	R	981.5	817.9	817.9	600.0	O
	#9	R	750.0	625.0	625.0	600.0	O
	#13	R	743.6	619.7	619.7	600.0	×
Site -2	#2	R	744.8	620.7	620.7	600.0	O
	#3	R	809.5	674.6	674.6	600.0	O
	#7	R	512.2	426.8	426.8	600.0	×
	#12	R	657.3	547.7	547.7	600.0	×
	#13	R	676.7	563.9	563.9	600.0	×

Note 1) DFI; Deep Foundation Institute, the US

Perko; Helical pile design and installation

A.P.C; Australian Piling Code

4. Suggestion of Equation for Calculating Bearing Capacity

4.1 Suggestion of Equation for Calculating Bearing Capacity According to Load Test Result

The helical plate and the pile tip penetrated into the location higher than the weathered soil (N>50) planned for the test installation in this study, and the piles penetrated even into the weathered rock top in the differential weathered layer of Site-1(#1-8). Moreover, the presence of gravity grout should be known to classify the equation for calculating bearing capacity depending on skin friction changes, and it is necessary to use an appropriate calculation equation after examining the stratum configuration in the pile installation site for classifying the end support layer.

4.1.1. Analysis of Skin Friction and Point Bearing Capacity According to Load Test Result

The load transfer test is required to examine the bearing capacity in which skin friction and point bearing capacity is classified to determine an equation for calculating bearing capacity. However, because small-diameter steel pipes of the helical piles are installed through rotary penetration, it is impossible to install the lead line of the strain gauge attached to the steel pipes for the load transfer test, and the load transfer test was thus not conducted in this study.

Therefore, with the extreme bearing capacity of the static load test as a true value in this study, it was planned to separate skin friction from point bearing capacity in consideration of the ratio of the cylindrical surface to the point bearing capacity in the dynamic pile load test conducted for the same piles. Therefore, the used data are for 4 pile samples of #7, #8 and #9 in Site-1 and #7 in Site-2.

Table 4 illustrates the extreme bearing capacity according to the static load test result, and Table 5 illustrates the ratio of skin friction to point bearing capacity according to the dynamic pile load test result. Table 6 illustrates skin friction and point bearing capacity according to the result illustrated in Tables 4 and 5. The skin friction according to the dynamic pile load test result is just for the shaft section, and the bearing capacity by the point tip and the helix plate is divided by means of the point bearing capacity.

Table 4. Extreme bearing capacity according to static load test result.

Pile No.	Point support layer	Grout	Extreme bearing capacity (kN)	Remarks
Site-1(#7)	Weathered soil	No	1,106.6	
Site-1(#8)	Weathered rock	Yes	At least 1,600.0	
Site-1(#9)	Weathered soil	Yes	1,356.0	
Site-2(#7)	Weathered soil	No	1,108.3	

Table 5. Ratio of skin friction to point bearing capacity according to dynamic pile load test result.

Pile No.	Allowable bearing capacity(kN)		Bearing capacity ratio		Remarks
	Skin friction	Point bearing capacity	Skin friction	Point bearing capacity	
Site-1(#7)	13.1	490.4	2.6%	97.4%	
Site-1(#8)	104.1	713.9	12.7%	87.3%	
Site-1(#9)	79.7	545.3	12.7%	87.3%	
Site-2(#7)	7.4	419.4	1.7%	98.3%	

Table 6. Classification of skin friction and point bearing capacity with load test result.

Pile No.	End support layer	Grout	Extreme bearing capacity(kN)		Remarks
			Skin friction	Point bearing capacity	
Site-1(#7)	Weathered soil	No	28.8	1,077.8	
Site-1(#8)	Weathered rock	Yes	203.2	At least 1,396.8	
Site-1(#9)	Weathered soil	Yes	172.2	1,183.8	
Site-2(#7)	Weathered soil	No	18.8	1,089.5	

4.1.2. Analysis of Design Standard

In other countries, the calculation equation suggested by [5] is the only equation known for calculating empirical bearing capacity according to the analysis result of load test data for helical pile installation, and Table 7 illustrates the equation.

Table 7. Perko (2009)'s equation for calculating bearing capacity.

Category	Equation for calculating bearing capacity	Remarks

Preprints (www.preprints.org) | NOT PEER-REVIEWED | Posted: 31 July 2018 doi:10.20944/preprints201807.0617.v1

Peer-reviewed version available at Materials 2018, 11, 1890; doi:10.3390/ma11101890

Ⓐ	Point bearing capacity	$q_P = \beta \times \lambda_{SPT} \times An$ β = bearing capacity coefficient Clay : 11, sand: 12, weathered rock : 13 λ_{SPT} = 6.2kPa/Blow Count(N) An : helix plate area	⇒ Equation for calculating point bearing capacity for each stratum Clay=68.2 × N × An Sand=74.4 × N × An Weathered rock=80.6 × N × An
	Cylindrical surface Friction	$q_s = \alpha \times H \times (\pi \times d)$ α = skin friction coefficient Non-grout = 2/3×T Grout = T	H = shaft length experiencing cylindrical surface friction d = pile diameter $T = 0.09e^{0.08Ø} \times \sigma'v \times \tan Ø$ $\sigma'v$ = effective horizontal stress Ø = internal friction angle

In Korea, the method for calculating point bearing capacity and skin friction depends on the method of installing pile foundations, in accordance with the applied standards of [23, 24].

The aforementioned design standards classify piles into 1) Driven pile, 2) Precast pile and 3) Cast-in-place concrete pile depending on the method of installation. In particular, conventional pile materials of PHC and steel pipe piles are used to manufacture the driven and precast piles, and used materials are determined in consideration of characteristics of the top load. In particular, the PHC piles are generally used where the top load is generally a vertical load, and steel pipe piles are used where the top load has vertical forces, moment and horizontal forces at the same time.

Therefore, for the conventional piles of PHC and steel pipes, weathered rocks or rock beds are selected as a support layer because it is necessary to select the method of installation and the support layer to maximize the use of allowable strength of the piles in consideration of load characteristics to ensure cost effectiveness.

Table 8 illustrates characteristics depending on the installation method and the equations for calculating bearing capacity.

Table 8. Characteristics depending on installation method and equations for calculating bearing capacity.

Category	Installation method	Support layer	Equation for calculating extreme bearing capacity		
Driven pile	Conventional piles are installed by using a drop or hydraulic hammer.	Rock bed equivalent to at least weathered rock	Ⓑ	End	$q_P = 300 \times N \times Ap$
				Cylindrical surface	$q_s = 2.0 \times N \times As$
Precast pile	A boring machine is first used to bore the ground and the pile is inserted and then driven.	Rock bed equivalent to at least weathered rock	Ⓒ	end	$q_P = (200 \sim 250) \times N \times Ap$
				Cylindrical surface	$q_s = (2.0 \sim 2.5) \times N \times As$
	A boring machine is first used to mix the		Ⓓ	End	$q_P = 150 \times N \times Apd$

Preprints (www.preprints.org) | NOT PEER-REVIEWED | Posted: 31 July 2018 doi:10.20944/preprints201807.0617.v1

Peer-reviewed version available at Materials 2018, 11, 1890; doi:10.3390/ma11101890

	end with grout and the pile is inserted.			Cylindrical surface	$q_s = (2.0 \sim 2.5) \times N \times As$ **Application : $q_s = 1.0 \times N \times As$**
Cast-in-place concrete pile	A boring machine is first used to bore the ground, and the reinforced steel net and concrete are then laid to install the pile.	Earth and sand ~ rock bed (earth and sand type is applied)	Ⓔ	End	$q_P = 100 \times N \times Ap$
				Cylindrical surface	$q_s = (3.3 \sim 5.0) \times N \times As$ **Application: $q_s = 5.0 \times N \times As$**

4.1.3. Application of Design Standard for Establishing Equation for Calculating Bearing Capacity

The equation for calculating bearing capacity of helical piles was established after examining appropriateness of conventional equations by comparing point bearing capacity and skin friction according to the result of the dynamic load test and the static load test with the extreme bearing capacity calculated with the calculation equation by [5] (Ⓐ) and the equations Ⓓ and Ⓔ based on Korean design standards.

Conventional equation Ⓐ: the base rock which is as a support layer is different but it is the same installation method; equations Ⓓ and Ⓔ: the installation method is different, but the method for calculating bearing capacity for the same support layer (base rock) is applied to analysis and comparison to establish an equation for calculating bearing capacity.

Table 9 illustrates comparison of the skin friction and point bearing capacity according to the load test with the end and skin friction calculated with the conventional equations. Table 10 illustrates the equations for calculating bearing capacity obtained from this experiment by using the result illustrated in Table 9. For the skin friction in the bearing capacity equations for the precast pile, 1.0× N was applied in consideration of the load test result, and the piles No. 1-8 supported with the weathered rock in the differential weathered layer are expected to have greater point bearing capacity. In consideration of this, the calculation equation was determined.

Table 9. Comparison of end and skin friction.

Category			**Pile No.**			
			1-7	**1-8**	**1-9**	**2-7**
Skin friction	Load test (①)		28.8kN	203.2kN	172.2kN	18.8kN
	Conventional equation	Ⓐ	55.7kN	99.2kN	98.0kN	50.2kN
		Ⓓ	**28.8kN**	40.8kN	40.5kN	**20.6kN**
		Ⓔ	144.1kN	**204.1kN**	**202.6kN**	102.9kN
	Ratio (%)	Ⓐ/①	193.4%	48.8%	56.9%	267.0%
		Ⓓ/①	100.0%	20.1%	23.5%	109.6%
		Ⓔ/①	500.3%	100.4%	117.7%	547.3%
	Result of examination		Similar to result of equation D	Similar to result of equation E	Similar to result of equation E	Similar to result of equation D
Point bearing capacity	Load test (①)		1,077.8kN	At least 1,396.8kN	1,183.8kN	1,089.5kN
		Ⓐ	869.5kN	830.8kN	830.3kN	874.8kN

Preprints (www.preprints.org) | NOT PEER-REVIEWED | Posted: 31 July 2018 doi:10.20944/preprints201807.0617.v1

Peer-reviewed version available at Materials 2018, 11, 1890; doi:10.3390/ma11101890

Conventional equation	Ⓓ	1,618.2kN	**1,545.3kN**	1,545.3kN	1,628.1kN
	Ⓔ	**1,078.8kN**	1,030.2kN	**1,030.2kN**	**1,085.4kN**
Ratio (%)	Ⓐ/①	80.7%	59.4%	70.1%	80.3%
	Ⓓ/①	150.1%	110.6%	130.5%	149.4%
	Ⓔ/①	100.1%	73.8%	87.0%	99.6%
Result of examination		Similar to result of equation E	Similar to result of equation D	Similar to result of equation E	Similar to result of equation E
Bearing capacity equation reliability		100.1%	109.3%	90.9%	99.8%

Table 10. Equation for calculating bearing capacity of helical pile.

Category	Point bearing capacity (kN)	Skin friction (kN)	Remarks
Support by weathered soil +Non-grout	$q_p=100\times N\times Ap$	$q_s=1.0\times N\times As$	N : SPT result Ap : Average area of helix plate As : Circumference of semi-hollow shaft
Support by weathered soil +grout		$q_s=5.0\times N\times As$	
Support by weathered rock +grout	$q_p=150\times N\times Ap$		

4.2 Equation for Calculating Bearing Capacity Considering Relation between Torque (T) and Extreme Bearing Capacity

4.2.1. Data Analysis

The analysis of relation between torque (T) and extreme bearing capacity aimed to enhance reliability of T-qu relation by analyzing torque (T) and extreme bearing capacity (qu) of the piles that underwent the static load test .

The following were applied to this study, that is, STK490, selection of steel pile of Ø165.2-7.5t, helix plate specifications of Ø350~450mm and gravity grout. Therefore, the aforementioned materials were used to ensure the target vertical bearing capacity of 600.0kN, and Table 11 and Figure 7 show the measured final torques and extreme bearing capacity.

Table 11. Measured torque (T) and extreme bearing capacity (q_u).

Pile No.	Installation method	Final torque (T, kN-m)	Extreme bearing capacity (q_u , kN)	Remarks
1-7	Rotary penetration	30.9	1,106.6	Non-Grout
1-8	Rotary penetration +Grout	29.5	At least 1,600	Increased friction by gravity grout
1-9	Rotary penetration +Grout	30.6	1,356.0	

Preprints (www.preprints.org) | NOT PEER-REVIEWED | Posted: 31 July 2018 doi:10.20944/preprints201807.0617.v1

Peer-reviewed version available at Materials 2018, 11, 1890; doi:10.3390/ma11101890

2-7	Rotary penetration	28.6	1,108.3	Non-Grout
2-8	Rotary penetration +Grout	31.0	1,329.3	Increased friction by gravity grout
2-9	Rotary penetration +Grout	29.8	1,254.6	

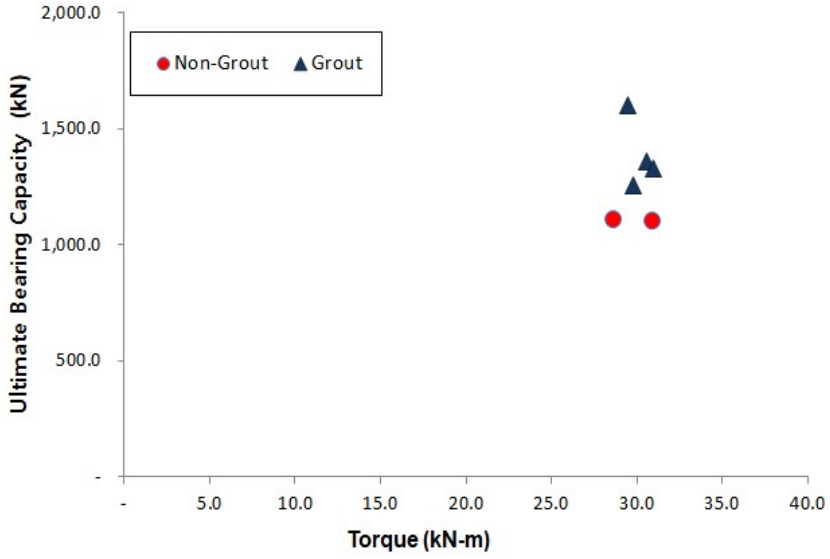

Figure 7. Torque (T)-extreme bearing capacity (q_u).

4.2.2. Bearing capacity coefficient (kt) according to the analysis of relation between torque (T)-extreme bearing capacity (qu)

For the analysis of relation between torques (T)-extreme bearing capacity (qu), the piles were divided into non-grout piles and grout piles to determine the bearing capacity coefficient (kt).

The analysis shows that vertical bearing capacity quality control of all piles is implemented and the reliability of vertical bearing capacity can be enhanced for the empirical bearing capacity coefficient kt because the vertical bearing capacity of the piles installed in the sites is known. In addition, the bearing capacity coefficient (kt) obtained from the non-grout piles and the grout piles can be used as illustrated in equations 1 and 2.

$$qut(kN) = T \times kt \quad (1)$$

$$qat(kN) = qut / Fs \quad (2)$$

in which qut : extreme vertical bearing capacity (kN) by kt;
qat : allowable vertical bearing capacity (kN) by kt;
T : final torque (kN·m) measured during installation;
kt : bearing capacity coefficient(m-1); and
Fs : safety factor (=2, based on AC358).

Tables 12, 13 and Figure 8 show the result of analysis of relation between torque (T)-extreme bearing capacity (qu) for the non-grout piles and grout piles.

Table 12. T-q_u analysis result for non-grout piles.

Pile No.	Torque (T, kN·m)	kt (m^{-1})	Extreme bearing capacity (kN)		Bearing capacity ratio (ⓑ/ⓐ)
			Measurement	Calculation	

Preprints (www.preprints.org) | NOT PEER-REVIEWED | Posted: 31 July 2018 doi:10.20944/preprints201807.0617.v1

Peer-reviewed version available at Materials 2018, 11, 1890; doi:10.3390/ma11101890

			static load test result ⓐ	qut=T×kt ⓑ	
1-7	30.9	35.8	1,106.6	1,106.2	100%
2-7	28.6	38.7	1,108.3	1,106.8	99.9%
Analysis result	The analysis of relation between T-qu for the non-grout piles shows that kt=35.8m^{-1} is applicable to weathered soil support piles.				

Table 13. T-q_u analysis result for grout piles.

Pile No.	Torque (T, kN-m)	kt (m^{-1})	Extreme bearing capacity(kN)		Bearing capacity ratio (ⓑ/ⓐ)
			Measurement	Calculation	
			static load test result ⓐ	qut=T×kt ⓑ	
1-8	29.5	54.2	At least 1,600	1,598.9	99.9%
1-9	30.6	44.3	1,356.0	1,355.6	99.8%
2-8	31.0	42.8	1,329.3	1,326.8	99.8%
2-9	29.8	42.0	1,254.6	1,251.6	99.8%
Analysis result	The analysis of relation T-qu for the grout piles shows that kt=554.2m^{-1} is applicable to weathered rock support piles and kt=42.0m^{-1} to the weathered soil support piles.				

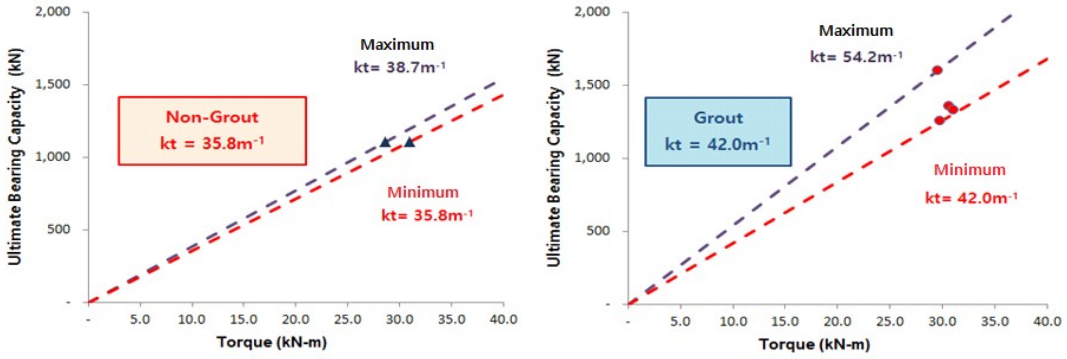

(a) (b)

Figure 8. Result of analysis of relation between torque (T)-extreme bearing capacity (q_u): (a) Non-grout pile; (b) Grout pile.

5. Summary and Conclusion

This study aims to improve the hollow shaft model to be a hexagon joint and a type not requiring welding or bolts in compressive loading. The following conclusion is drawn by analyzing the static load test result through the field test, dynamic pile load test, and comparing the bearing capacity estimated with measured torque to apply the method to Korean ground.

1. The analysis result of the static load test through the field pile load test shows the allowable bearing capacity of the gravity grout piles was 678.6~800kN/pile in Site-1 and 627.3 ~664.7kN/pile in Site-2. The allowable bearing capacity of the non-grout piles was smaller than the target load of 600.0kN/pile in both Sites-1 and 2, suggesting gravity grouting is required to install helical piles. Moreover, the target load of 600.0kN resulted in 1 inch (25.4mm) which is the allowable settlement standard, suggesting stability in settlement.

2. The analysis of the dynamic pile load test through the field pile load test shows that the allowable bearing capacity of the gravity grout piles was 625.0~817.9kN/pile in Site-1 and 620.7~674.6kN/EA in Site-2. The allowable bearing capacity of the non-gravity-grout piles was smaller than 600.0kN/pile in Sites-1 and 2, similar to the static load test result.

3. In the result with the equation for calculating the empirical bearing capacity in consideration of the load test result, the point bearing capacity (kN) of weathered soil support + non-grout and grout piles was q_p=100×N×Ap, and the point bearing capacity(kN) of the weathered rock support + grout piles was q_p=150×N×Ap. Moreover, the skin friction (kN) of the weathered soil support + non-grout piles was q_s=1.0×N×As, and the skin friction (kN) of the weathered soil support and weathered rock support + grout piles was q_s=5.0×N×As. The equation for calculating the empirical bearing capacity was established with a small number of samples, and can be used as basic data.

4. With the equation for calculating bearing capacity in consideration of torque (T) during pile installation, the bearing capacity coefficient (kt) of non-grout piles was 35.8m^{-1}, allowing quality control; the bearing capacity coefficient (kt) of the weathered soil support + grout piles was 42.0m^{-1}; and the bearing capacity coefficient (kt) of the weathered rock support piles was 54.2m^{-1}, allowing quality control. The equation for calculating the bearing capacity in consideration of torque (T) was established with a small number of samples as for the empirical bearing capacity, and can be used as basic data.

Author Contributions: Writing-Original Draft Preparation, D. Kim and K. Baek; Writing-Review & Editing, K. Park.

Acknowledgments: This study was supported by research funds from Chosun University, 2015.

Conflicts of Interest: The authors declare no conflict of interest.

References

1. Livneh, B.; Naggar, M.H. Axial Testing and Numerical Modeling of Square Shaft Helical Piles under Compressive and Tensile Loading, *Canadian Geotehnical Journal*, **2008**, *45*, 1142-1155, https://doi.org/10.1139/T08-044
2. Yoo, C.S. Effect of Screw Geometries on Pull-out Characteristics of Screw Anchor Piles Using Reduced Scale Model Tests, *Journal of the Korean Geotechnical Society*, **2012**, *28*, 5-15.
3. Ha, T.S.; Moon, H.R.; Moon, H.M. An Analysis of Correlation between Predicted and Measured Bearing Capacity in Rotary(Helical) Pile Method, *KGS Fall National Conference 2013*, Gyeonggi, Korea, October 17, 2013, 694-699.
4. Lee, J.W. Study on Relationship between Configuration of Helical Pile and Bearing Capacity, Master Degree, Korea University, Seoul, Korea, August 28, 2014.
5. Perko, H.A. *Helical Piles: A Practical Guide to Design and Installation*, John Wiley and Sons, New York, USA, 2009; pp. 103-215, ISBN 978-0-470-40479-9.
6. Mitsch, M.P.; Clemence, S.P. *The Uplift Capacity of Helix Anchors and Sand*, American Society of Civil Engineering, New York, USA, 1985; pp. 26-47, ISBN 978-0-87262-496-2.
7. Dames; Moore, *Pullout Test on Multi Helix Anchors*, A report prepared for Virginia Power Company, Shacklefords, Virginia, USA, 1990.
8. Clemence, S.P. *Uplift Behavior of Anchor Foundations in Soil*, American Society of Civil Engineering, New York, USA, 1985; pp. 1-126, ISBN 978-0-87262-496-2.
9. Mooney, J.S.; Adamczak Jr., S.; Clemence, S.P. Uplift Capacity of Helix Anchors in Clay and Silt, In Proceedings of ASCE Convention, Detroit, Michigan, USA, 1985; 48-72.
10. Narasimha, R.S.; Prasad, Y.V.S.N.; Shetty, M.D. The Behavior of Model Screw Piles in Cohesive Soils, *Soils and Foundations*, **1991**, *31*, 35-50, https://doi.org/10.3208/sandf1972.31.2_35

11. Merifield, R.S.; Smith, C.C. The Ultimate Uplift Capacity of Multi-plate Strip Anchors in Undrained Clay, *Computers and Geotechnics*, **2010**, *37*, 504–514, https://doi.org/10.1016/j.compgeo.2010.02.004
12. Seider, G. Eccentric Loading of Helical Piers for Underpinning, *Proceedings of The 3rd International Conference on Case Histories in Geotechnical Engineering*, St. Louis, Missouri, USA, June 1-4, 1993; Paper No. 1.37, 139-145.
13. Ghaly, A.M. and Clemence, S.P. Pullout Performance of Inclined Helical Screw Anchors in Sand, *Journal of Geotechnical and Geoenvironmental Engineering*, **1998**, *124*, 617-627, https://doi.org/10.1061/(ASCE)1090-0241(1998)124:7(617)
14. Narasimha, R.S.; Prasad, Y.V.S.N.; Veeresh, C. Behavior of Embedded Model Screw Anchors in Soft Clays, *Geotechnique*, **1993**, *43*, 605-614, https://doi.org/10.1680/geot.1993.43.4.605
15. Hoyt, R.M.; Clemence, S.P. Uplift Capacity of Helical Anchors in Soil, *12th International Conference on Soil Mechanics and Foundation Engineering*, Conducted in Rio de Janeiro, Brazil, 1989, 1019-1022.
16. Perko, H.A. Energy Method for Predicting the Installation Torque of Helical Foundations and Anchors, New Technological and Design Developments in Deep Foundations, Denver, Colorado, USA, 2000, 342-352.
17. Lee, D.; Na, K.; Lee, W.; Kim, H.; Choi, H. Applicability of Bi-directional Load Test for Evaluation Bearing Capacity of Helical Piles, *Journal of Korean Geosynthetics Society*, **2014**, *13*, 77-85, http://dx.doi.org/10.12814/jkgss.2014.13.4.077
18. Park, K.H.; Kim, K.B. The Behavior Characteristics of Bearing Capacity using The Helical Pile was settled in Rock, *KSCE National Conference 2015*, Seoul, Korea, October 29-30, 2015, 37-38.
19. Lee, B.J.; Lee, J.K. A Case Study on the Construction of Helical Pile, *KGS Fall National Conference 2016*, Gyeonggi, Korea, October 23, 2016, 61-62.
20. AC358 *Acceptance Criteria for Helical Foundation Systems and Devices*, ICC Evaluation Service, INC., California, USA, 2007; pp. 1-21.
21. Andina, S.; Leonids, P. Helical Pile Behavior and Load Transfer Mechanism In Different Soils, *The 10th International Conference Modern Building Materials*, Structures *and Techniques*, Vilnius, Lithuania, 2010, 1174-1180.
22. Chance Civil Construction, *Technical Design Manual*, Hubbell Power Systems, Inc., Missouri, USA, 2014; pp. 304-335.
23. Korea Geotechnical Society, *Guidelines for Structure Foundation Design*, Seoul, Korea, 2008; pp. 316-322.
24. Ministry of Construction and Transportation, Guidelines for Road Bridge Design, Seoul, Korea, 2015; pp. 856-870.